Paramagnetic Relaxation Enhancement Reveals Oligomerization Interface of a Membrane Protein

Shenlin Wang,[†] Rachel A. Munro,[†] So Young Kim,[‡] Kwang-Hwan Jung,[‡] Leonid S. Brown,*,[†,§] and Vladimir Ladizhansky*,[†,§]

[†]Department of Physics and [§]Biophysics Interdepartmental Group, University of Guelph, Guelph, Ontario, Canada
[‡]Department of Life Science and Institute of Biological Interfaces, Sogang University, Seoul, Korea

Ⓢ Supporting Information

ABSTRACT: Protein−protein interactions play critical roles in cellular function and oligomerization of membrane proteins is a commonly observed phenomenon. Determining the oligomerization state and defining the intermolecular interface in the bilayer is generally a difficult task. Here, we use site-specific spin labeling to demonstrate that relaxation enhancements induced by covalently attached paramagnetic tag can provide distance restraints defining the intermonomer interface in oligomers formed by a seven-helical transmembrane protein *Anabaena* Sensory Rhodopsin (ASR). We combine these measurements with visible CD spectroscopy and cross-linking experiments to demonstrate that ASR forms tight trimers in both detergents and lipids.

Many membrane proteins show high propensity to oligomerize. While for some membrane proteins the oligomerization is undisputedly critical for their function, for example, for ion channels, for many others the oligomerized states found in crystals or in detergent micelles may actually be promoted by the environment. The ability to oligomerize may be very different in the environment of a lipid bilayer and can be further modulated by its various characteristics such as protein crowdedness and bilayer fluidity. Furthermore, in the cellular environment, the presence of other proteins may also play a role. Solid-state NMR has been extensively used in recent years to characterize structures of membrane proteins in lipid environments,[1−4] and more recently in the heterogeneous native membranes or in whole cells.[5−7] The technique is capable to report on intermolecular packing, either in crystals,[8−11] amyloids,[12] or membranes,[13,14] but is generally limited by the scarcity of long-range internuclear distance restraints. Electron−nuclear interactions, on the other hand, can be used to monitor longer distances and are actively used for structure determination in both solution- and solid-state NMR.[15−17] The effect of Paramagnetic Relaxation Enhancement (PRE) can provide unambiguous long-range restraints even when combined with simple 2D spectroscopy,[18] and is more suitable for the identification of interaction interfaces. Furthermore, paramagnetic restraints in the solid state can be used to derive accurate distance restraints[19−25] and to determine protein structures by SSNMR.[26−30]

Here, we present a magic-angle spinning (MAS) SSNMR study of oligomers formed by a seven-helical membrane-associated *Anabaena* Sensory Rhodopsin (ASR) in lipids. ASR is a unique cyanobacterial photosensor, believed to be responsible for chromatic adaptation.[31] Its X-ray structure has been solved to 2 Å resolution.[32] Solid-state NMR assignments and its refined structural model were reported previously and revealed a number of structural differences between ASR in lipids and in crystals.[33] Here, we show that intermolecular PREs observed by SSNMR define the oligomerization surface, which is drastically different from intermolecular contacts observed in crystals. PRE data alone is not sufficient to determine oligomeric order, so we combined NMR with additional biochemical measurements to demonstrate that ASR forms trimers in lipids.

There are several lines of experimental evidence suggesting that ASR forms oligomers. ASR solubilized in *n*-dodecyl-*β*-D-maltopyranoside (DDM) micelles forms large protein-detergent complexes of ∼600 kDa.[34] Nondenaturing SDS-PAGE (Figure S4) shows that a significant portion of ASR runs as a high molecular weight complex at approximately 60 kDa, which corresponds to trimers (monomers run at ∼20 kDa). This band disappears in the samples boiled with SDS. While this cannot serve as a proof that ASR indeed forms trimers in the membranes, it nevertheless suggests such a possibility. The second piece of evidence comes from visible CD spectroscopy. In homologous BR, visible CD spectra have a characteristic bilobe shape, which was shown to correlate to trimer formation.[35] The CD spectra of ASR in DDM micelles and lipids have very similar shape (Figure S6) indicating trimerization in both the detergent and lipid environments. Third, cross-linking experiments conducted in both DDM micelles and in lipids show the presence of trimers (see Figure S5 for details). Trimerization of ASR is not surprising in view of its strong homology with BR and halorhodopsin, both of which form trimers.[36,37] It should be noted that ASR trimers are more stable than those in BR, which are easily destroyed by detergent solubilization.[38]

To obtain intermolecular distance constraints and to characterize the oligomerization interface of ASR, we used PRE on samples with nitroxide labels attached to cysteine side chains introduced into the wild-type background (for reasons discussed below) at the potential oligomerization interface. We used S24C and S26C mutants with conservative replacements

of serines on the cytoplasmic end of helix A (for details of sample preparation see Supporting Information (SI)). The locations of the mutations were chosen based on the known structure of the BR trimer, in which the A–B pair of helices from one monomer is facing the D–E pair of helices of its neighbor.[39,40] We chose to place the labels on helix A rather than B, as B is expected to be in much tighter contact with the helix D of the next monomer, which could create steric clashes and either prevent labeling or disrupt oligomerization.

Introduction of non-native cysteines into the wild-type background is safe for selective labeling in ASR. Wild-type ASR contains three native intramembrane cysteine residues at positions 134 and 137 in helix E, and 203 in helix G (see Figure S3 for amino acid sequence), none of which is accessible to the (1-oxyl-2,2,5,5-tetramethyl-Δ3-pyrroline-3-methyl) methanethiosulfonate (MTSL) reagent. To verify this, we attempted to attach a diamagnetic label with similar cysteine reactivity, methyl methanethiosulfonate (MMTS), using reaction conditions identical to those for MTSL labeling (see SI for details). Both the chemical shifts of the CA and CB cysteine atoms of the reaction product, and the relative intensities of CA/CB cross peaks remained unchanged (Figure S3), indicating that all three native cysteines were nonreactive.

On the basis of the X-ray structure[32] and the revised SSNMR model of ASR,[33] the side chains of both S26 and S24 are located on the external protein surface. Therefore, the MTSL side chains may point toward the intermonomer interface, provided that mutations do not introduce significant distortions in the secondary structure. Of the two cysteine mutants, only S26C could be labeled with MTSL, with C24 likely being protected. A direct comparison of solid-state NMR spectra between the wild-type and S26C mutant (Figure S2) reveals that the mutant retains essentially the same structure as the wild-type. NMR PRE measurements were performed on the S26C mutant with a paramagnetic nitroxide side-chain (R1), and on the diamagnetically (MMTS) labeled control sample, R1′, referred as S26CR1 and S26CR1′ in the following. Two kinds of samples were prepared for PRE measurements. In the first, isotopically labeled S26CR1 was diluted in a ratio of 1:2 with natural abundance S26CR1′, and in the second isotopically labeled S26CR1 was used without dilution. As shown in the following, the introduction of paramagnetic label in S26CR1 causes significant intermonomer PRE effects, which were identified through site-specific measurements of PREs, and through the analysis of intramonomer distances between the free radical and the strongly affected residues. The results obtained for diluted and undiluted samples were similar (Figure S7), indicating that oligomers found in micelles are strong, and are not disrupted by the lipid reconstitution process. Additionally, it also suggests the absence of appreciable inter-trimer PRE effects.

The presence of a covalently attached paramagnetic nitroxide enhances transverse relaxation and is expected to result in disappearance or strong attenuation of signals from residues in close proximity to the paramagnetic label.[18] A comparison of 2D NCA spectra (Figure 1) of paramagnetically and diamagnetically labeled samples reveals that peaks from many residues either disappear or are significantly attenuated in the former.

Site-specific comparison of cross peak intensities in Figure 2 shows strong attenuation in the cytoplasmic sides of helices A and B and in the A–B loop (residues 18–44) which are in close proximity to the paramagnetic label attached to C26.
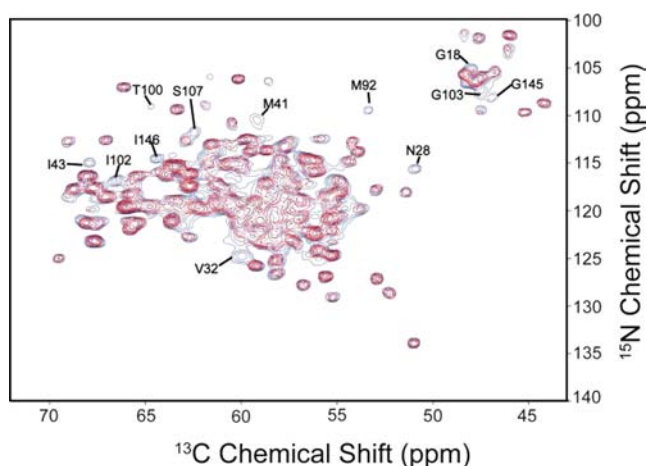
Figure 1. 800 MHz 2D NCA correlation spectra of paramagnetically labeled S26CR1 (red) and its diamagnetic control S26CR1′ (blue). Some of the affected residues are labeled.
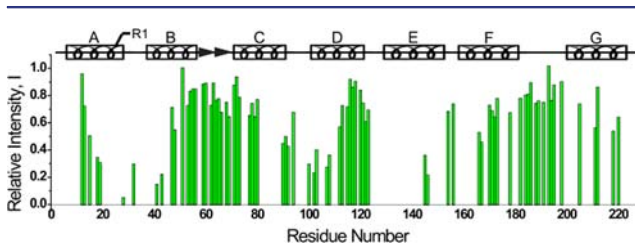

Figure 2. Site-specific comparison of relative cross peak intensities in NCA experiments recorded in S26CR1 and S26CR1′ samples. To account for possible small variations in the amount of sample, the ratios were normalized as $I = (I_{para}/I_{dia})/(I_{para}/I_{dia})_{max}$, where I_{para} and I_{dia} are the peak heights in the NCA spectra of S26CR1 and S26CR1′ samples, respectively, and $(I_{para}/I_{dia})_{max}$ is the maximal I_{para}/I_{dia} value. Secondary structure of ASR with indicated position of the paramagnetic label is shown on top.

Additionally, strongly affected residues are located in the C–D loop, and in the cytoplasmic half of helix D (positions 100–108), as well as near the cytoplasmic end of helix E (residues 145 and 146). As expected, residues on the extracellular side are among the least affected by the paramagnetic labeling.

As many cross-peaks are not individually resolved in the 2D NCA spectra, additional PREs were obtained from the comparison of 2D $^{13}C–^{13}C$ correlation spectra recorded in the S26CR1 and S26CR1′ samples (Figure S9). Overall, we observed similar trends: signals from residues in the cytoplasmic halves of helices A, B, D, E, and A–B and C–D loops were attenuated indicating close proximity to the paramagnetic center, while minimal effects were observed on the extracellular side. Additionally, the ^{13}C data confirm the absence of paramagnetic labeling of the three native cysteines.

Amide protons of the strongly affected residues in helices A, B and in the A–B loop are all within 15 Å from the radical (Figure 3), consistent with theoretical estimations.[18] Quantitatively similar PRE effects were observed for helices D and E, which suggest that their affected protons are roughly within the same distance range from the paramagnetic center.
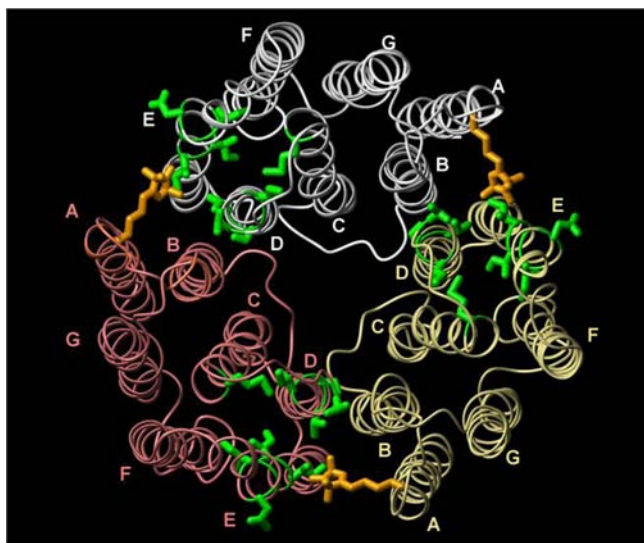
Attenuated signals in helices D and E cannot be explained by intramonomer interactions. Indeed, amide protons of the affected residues 100–110 in helix D and 145–146 in helix E are too far from the paramagnetic label, ~25 Å or longer (Figure 3). Furthermore, even if one assumes that, contrary to
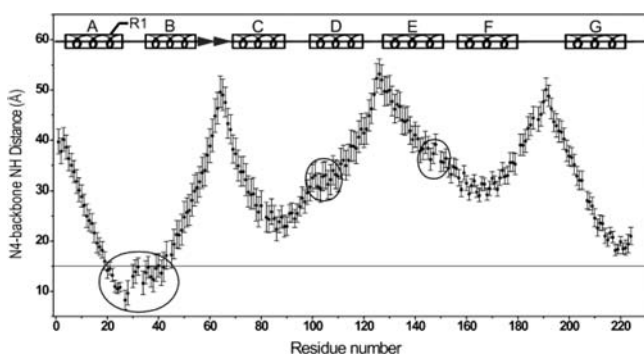
Figure 3. Estimated distances between the nitroxide spin label and backbone amide protons in S26CR1. Circles highlight the regions with large PRE effects with relative NCA cross peak intensities less than 0.33. The straight line at the position of 15 Å is shown to guide the eye. Error bars in distance estimation result from the uncertainty of the MTSL geometry. More details are given in SI.

the expectations from known ASR structure, the paramagnetic label point to the protein interior, the neighboring helices G, C, and F should show strong PRE effects, which is clearly not the case (Figures 2, S9). Thus, the observed PRE effects in helices E and D must be from intermolecular interactions between neighboring ASR molecules. Similar magnitudes of PRE effects observed in diluted and undiluted samples point out that trimers of ASR detected in detergent micelles are not disrupted by the lipid reconstitution process.

The combined NCA (Figure 2) and $^{13}C-^{13}C$ (Figure S9) PRE data identify the residues with the backbone and/or side chain atoms close to the neighboring monomer, and define the oligomerization interface, which can be readily visualized on the trimer model (Figure 4), built as described in SI. It is clear that the oligomerization interface defined from the PRE data makes perfect structural sense in the case of the BR-like ASR trimer, in which the proximity of helix A of one monomer to helices D

and E of the other monomer is expected. This arrangement of monomers and the respective oligomerization interface are dramatically different from the one observed in crystals, which contain undulating layers of dimers.[32] It should be noted that, even if no homology modeling is possible, PREs can still provide invaluable information on membrane protein oligomerization interface.

In conclusion, we have shown that PRE can be used to study oligomerization of membrane proteins in lipids, and to obtain semiquantitative distance restraints for structure calculations. For *Anabaena* Sensory Rhodopsin, PRE data were combined with CD spectroscopy, cross-linking and SDS-PAGE to provide evidence that ASR forms tight trimers in lipids. Two key advantages of using PRE effects in large proteins like ASR are that (i) PRE effects can be interpreted unambiguously even when combined with simple 2D spectroscopy, and (ii) they give access to information on medium-range distances critical for understanding intermolecular packing. Furthermore, more accurate quantification of relaxation rates in combination with the use of other paramagnetic tags, such as EDTA:Cu, may provide rather precise distance constraints for structure determination.[26] Such techniques, which employ paramagnetic tags to probe intermolecular interfaces will likely find widespread use for the analysis of protein−protein interactions.

■ ASSOCIATED CONTENT

Ⓢ Supporting Information
Sample preparation procedures, details of cross-linking experiments, control experiments, additional NMR spectra. This material is available free of charge via the Internet at http://pubs.acs.org.

■ AUTHOR INFORMATION

Corresponding Author
lebrown@uoguelph.ca; vladizha@uoguelph.ca

Notes
The authors declare no competing financial interest.

■ ACKNOWLEDGMENTS

Figure 4. Trimer model of S26CR1 ASR. The individual monomers are shown in different colors. R1 side chains are shown in orange. Side chains of residues experiencing large intermolecular PRE effects ($I < 0.33$ in either NCA or $^{13}C-^{13}C$ spectra) and therefore spatially close (<15 Å) to the nitroxide from neighboring monomer are shown in green.

■ REFERENCES

(1) McDermott, A. *Annu. Rev. Biophys.* **2009**, *38*, 385.
(2) Renault, M.; Cukkemane, A.; Baldus, M. *Angew. Chem., Int. Ed.* **2010**, *49*, 8346.
(3) Sharma, M.; Yi, M.; Dong, H.; Qin, H.; Peterson, E.; Busath, D. D.; Zhou, H. X.; Cross, T. A. *Science* **2010**, *330*, 509.
(4) Cady, S. D.; Schmidt-Rohr, K.; Wang, J.; Soto, C. S.; Degrado, W. F.; Hong, M. *Nature* **2010**, *463*, 689.
(5) Fu, R.; Wang, X.; Li, C.; Santiago-Miranda, A. N.; Pielak, G. J.; Tian, F. *J. Am. Chem. Soc.* **2011**, *133*, 12370.

(6) Renault, M.; Pawsey, S.; Bos, M. P.; Koers, E. J.; Nand, D.; Tommassen-van Boxtel, R.; Rosay, M.; Tommassen, J.; Maas, W. E.; Baldus, M. *Angew. Chem., Int. Ed.* **2012**, *51*, 2998.

(7) Renault, M.; Tommassen-van Boxtel, R.; Bos, M. P.; Post, J. A.; Tommassen, J.; Baldus, M. *Proc. Natl. Acad. Sci. U.S.A.* **2012**, *109*, 4863.

(8) Peng, X.; Libich, D.; Janik, R.; Harauz, G.; Ladizhansky, V. *J. Am. Chem. Soc.* **2008**, *130*, 359.

(9) Helmus, J. J.; Nadaud, P. S.; Hofer, N.; Jaroniec, C. P. *J. Chem. Phys.* **2008**, *128*, 052314.

(10) Jehle, S.; Rajagopal, P.; Bardiaux, B.; Markovic, S.; Kuhne, R.; Stout, J. R.; Higman, V. A.; Klevit, R. E.; van Rossum, B. J.; Oschkinat, H. *Nat. Struct. Mol. Biol.* **2010**, *17*, 1037.

(11) Nieuwkoop, A. J.; Rienstra, C. M. *J. Am. Chem. Soc.* **2010**, *132*, 7570.

(12) Wasmer, C.; Lange, A.; Van Melckebeke, H.; Siemer, A. B.; Riek, R.; Meier, B. H. *Science* **2008**, *319*, 1523.

(13) Lu, J. X.; Sharpe, S.; Ghirlando, R.; Yau, W. M.; Tycko, R. *Protein Sci.* **2010**, *19*, 1877.

(14) Can, T. V.; Sharma, M.; Hung, I.; Gor'kov, P. L.; Brey, W. W.; Cross, T. A. *J. Am. Chem. Soc.* **2012**, *134*, 9022.

(15) Jaroniec, C. P. *Solid State Nucl. Magn. Reson.* **2012**, *43−44*, 1.

(16) Gottstein, D.; Reckel, S.; Dotsch, V.; Guntert, P. *Structure* **2012**, *20*, 1019.

(17) Otting, G. *Annu. Rev. Biophys.* **2010**, *39*, 387.

(18) Nadaud, P. S.; Helmus, J. J.; Hofer, N.; Jaroniec, C. P. *J. Am. Chem. Soc.* **2007**, *129*, 7502.

(19) Nadaud, P. S.; Helmus, J. J.; Kall, S. L.; Jaroniec, C. P. *J. Am. Chem. Soc.* **2009**, *131*, 8108.

(20) Jovanovic, T.; McDermott, A. E. *J. Am. Chem. Soc.* **2005**, *127*, 13816.

(21) Balayssac, S.; Bertini, I.; Lelli, M.; Luchinat, C.; Maletta, M. *J. Am. Chem. Soc.* **2007**, *129*, 2218.

(22) Balayssac, S.; Bertini, I.; Bhaumik, A.; Lelli, M.; Luchinat, C. *Proc. Natl. Acad. Sci. U.S.A.* **2008**, *105*, 17284.

(23) Bertini, I.; Emsley, L.; Lelli, M.; Luchinat, C.; Mao, J.; Pintacuda, G. *J. Am. Chem. Soc.* **2010**, *132*, 5558.

(24) Parthasarathy, S.; Long, F.; Miller, Y.; Xiao, Y.; McElheny, D.; Thurber, K.; Ma, B.; Nussinov, R.; Ishii, Y. *J. Am. Chem. Soc.* **2011**, *133*, 3390.

(25) Luchinat, C.; Parigi, G.; Ravera, E.; Rinaldelli, M. *J. Am. Chem. Soc.* **2012**, *134*, 5006.

(26) Sengupta, I.; Nadaud, P. S.; Helmus, J. J.; Schwieters, C. D.; Jaroniec, C. P. *Nat. Chem.* **2012**, *4*, 410.

(27) Su, Y.; Hu, F.; Hong, M. *J. Am. Chem. Soc.* **2012**, *134*, 8693.

(28) Bertini, I.; Bhaumik, A.; De Paepe, G.; Griffin, R. G.; Lelli, M.; Lewandowski, J. R.; Luchinat, C. *J. Am. Chem. Soc.* **2010**, *132*, 1032.

(29) Knight, M. J.; Pell, A. J.; Bertini, I.; Felli, I. C.; Gonnelli, L.; Pierattelli, R.; Herrmann, T.; Emsley, L.; Pintacuda, G. *Proc. Natl. Acad. Sci. U.S.A.* **2012**, *109*, 11095.

(30) Knight, M. J.; Felli, I. C.; Pierattelli, R.; Bertini, I.; Emsley, L.; Herrmann, T.; Pintacuda, G. *J. Am. Chem. Soc.* **2012**, *134*, 14730.

(31) Jung, K. H.; Trivedi, V. D.; Spudich, J. L. *Mol. Microbiol.* **2003**, *47*, 1513.

(32) Vogeley, L.; Sineshchekov, O. A.; Trivedi, V. D.; Sasaki, J.; Spudich, J. L.; Luecke, H. *Science* **2004**, *306*, 1390.

(33) Shi, L.; Kawamura, I.; Jung, K. H.; Brown, L. S.; Ladizhansky, V. *Angew. Chem., Int. Ed.* **2011**, *50*, 1302.

(34) Kondoh, M.; Inoue, K.; Sasaki, J.; Spudich, J. L.; Terazima, M. *J. Am. Chem. Soc.* **2011**, *133*, 13406.

(35) Heyn, M. P.; Cherry, R. J.; Dencher, N. A. *Biochemistry* **1981**, *20*, 840.

(36) Henderson, R.; Unwin, P. N. *Nature* **1975**, *257*, 28.

(37) Sasaki, T.; Kubo, M.; Kikukawa, T.; Kamiya, M.; Aizawa, T.; Kawano, K.; Kamo, N.; Demura, M. *Photochem. Photobiol.* **2009**, *85*, 130.

(38) Dencher, N. A.; Heyn, M. P. *FEBS Lett.* **1978**, *96*, 322.

(39) Mitsuoka, K.; Hirai, T.; Murata, K.; Miyazawa, A.; Kidera, A.; Kimura, Y.; Fujiyoshi, Y. *J. Mol. Biol.* **1999**, *286*, 861.

(40) Grigorieff, N.; Ceska, T. A.; Downing, K. H.; Baldwin, J. M.; Henderson, R. *J. Mol. Biol.* **1996**, *259*, 393.

16998

dx.doi.org/10.1021/ja308310z | *J. Am. Chem. Soc.* 2012, 134, 16995−16998